Penerbit Akademia Baru

Journal of Advanced Research in Fluid Mechanics and Thermal Sciences

Journal homepage: www.akademiabaru.com/arfmts.html
ISSN: 2289-7879

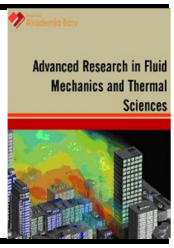

Application of Box-Behnken Design with Response Surface to Optimize Ventilation System in Underground Shelter

Open Access

Azfarizal Mukhtar[1,*], Mohd Zamri Yusoff[1], Khai Ching Ng[2], Mohamad Fariz Mohamed Nasir[3]

[1] Centre for Fluid Dynamics, College of Engineering, Universiti Tenaga Nasional (UNITEN), Putrajaya Campus, Jalan IKRAM-UNITEN, 43000 Kajang, Selangor, Malaysia
[2] School of Engineering, Taylor's University, Taylor's Lakeside Campus, No. 1, Jalan Taylor's, 47500 Subang Jaya, Selangor Darul Ehsan, Malaysia
[3] INTI International College, Menara KH, Jalan Sultan Ismail, Kuala Lumpur, 50250 Kuala Lumpur, Malaysia

ARTICLE INFO

Article history:
Received 9 September 2018
Received in revised form 16 October 2018
Accepted 2 November 2018
Available online 12 December 2018

Keywords:
CFD, Optimization, Box-Behnken Design, Response Surface, Ventilation Rate.

ABSTRACT

Ventilation shaft is one of the effective elements in natural ventilation for ensuring acceptable Indoor Air Quality (IAQ) and thermal comfort. It has been found that the opening of ventilation shaft plays a significant role in the ventilation efficiency of an underground shelter. In this study, we aim to develop a predictive ventilation rate model for a naturally-ventilated underground shelter. Computational Fluid Dynamics (CFD) was employed as a simulation tool, where the result was validated with experimental data obtained from the previous literature. Goal Driven Optimization (GDO) was used for the optimization process by considering three geometrical factors and their effects on the objective function. From this study, it is found that the predicted response surface values agree well with the CFD values and hence the predictive model is reliable.

1. Introduction

Providing a comfortable environment with better Indoor Air Quality (IAQ) for the occupant [1,2] is a fundamental criterion in designing a ventilation system of an underground building. In this regard, the design parameter such as ventilation rate is commonly used in IAQ analysis [3,4], indicating that a good ventilation system is equally important for an underground shelter. Obviously, an ill-designed ventilation system is detrimental to the health of indoor occupants. Thus, the IAQ of an underground shelter is dependent on the configuration of ventilation shaft.

In general, it can be noted that most underground shelters are equipped with a mechanical device [5] for better ventilation (instead of relying on natural ventilation). However, it is necessary to apply natural ventilation when the mechanical system fails [6–8]. Therefore, investigation on factors that could influence the ventilation effectiveness is necessary. Experimental studies [7,8] had been performed to improve the ventilation performance of an underground shelter. These

* *Corresponding author.*
E-mail address: azfarizal.mukhtar@gmail.com (Azfarizal Mukhtar)

studies, however, focused only on One-Factor-at-A-Time (OFAT) design without considering any other factors due to the limitation of the apparatus. This traditional method does not take into account the full effect of factors on the response.

In order to study the full effects of all factors, this study integrates the numerical optimization method with the CFD model. ANSYS Workbench (CFD) and ANSYS Design Exploration (GDO) were employed to develop a predictive ventilation rate model for a naturally ventilated underground shelter. Three design variables were considered, namely the inlet opening (m), the outlet opening (m) and the ratio of elbow shaft (R/H). The response variable is the ventilation rate. The case considered here was taken from King [8], in which careful verification and validation of the CFD model had been performed before the model was optimized by using the Box-Behnken design (BBD) and the full second-order polynomial of response surface (quadratic regression).

2. Methods

2.1 Computational Fluid Dynamics Modelling

The experimental data reported by [8] was used to validate the current CFD model. This building served as an emergency shelter which can be occupied by only one person (e.g. during war). A 3D CAD model of the shelter (used for simulation purpose) was given in Fig. 1. The rectangular region at the top of the shelter domain was used to model the atmospheric condition (above ground) of the physical experiment [9]. The walls of this rectangular region were placed away from the ventilation shafts of the underground shelter in order to minimise the wall effects due to the ventilation shafts. By applying this condition, airflow can be induced through the opening (i.e. inlet shaft) to mimic the real experimental conditions. The heating cable was designed to replicate the cooling load due to the occupant.

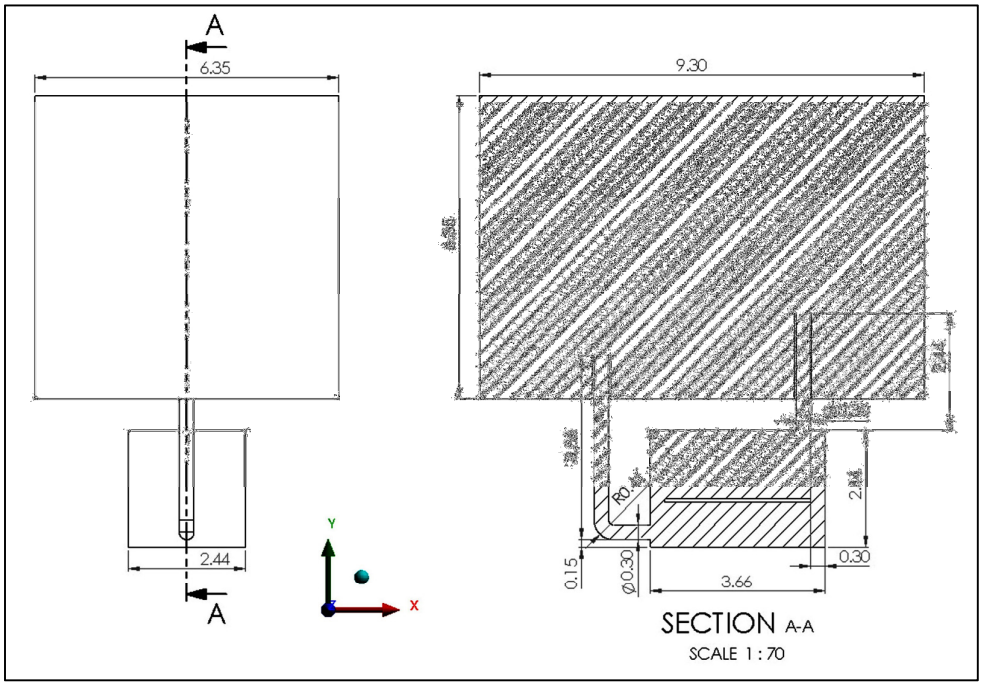

Fig. 1. 3D CAD replication

The airflow inside the shelter was considered as steady, incompressible and turbulent. The Finite Volume Method (FVM) was used to discretize the incompressible Reynolds-Averaged Navier-Stokes (RANS) equation. The equations were solved by using the pressure-based solver. There are a few turbulence models available in ANSYS Fluent, e.g. Spalart-Allmaras, $k-\varepsilon$, $k-\omega$, Shear Stress Transport (SST), Reynolds Stress, etc. Among these models, $k-\varepsilon$ model is commonly used as it is able to capture one or more flow features in indoor airflow, e.g. flow separation, thermal plume, jet flow, etc. [11] at reasonable accuracy [12]. In the current study, the realizable $k-\varepsilon$ model, i.e. an enhanced version of standard $k-\varepsilon$ model, was applied to model the flow turbulence. SIMPLEC was used for pressure-velocity coupling. Also, the use of higher-order convective schemes are essential to ensure flow accuracy (see [9,13]). Therefore, all governing equations were discretized using second-order upwind schemes for both accuracy and stability purposes. The sparse matrices were solved by using the Gauss-Seidel iterative solver and the Algebraic Multi-Grid (AMG) method was applied to accelerate the solution convergence. In this study, for convergence purpose, the flexible cycle was used in solving the energy equation. Lastly, the solution was executed for approximately 850 iterations to attain a converged solution. The solution was considered to be converged when there were no more obvious fluctuations in velocity, energy and the turbulence variables (the scaled residual RMS errors were less than 10^{-4}) and the domain has net imbalance of less than 1%. After the simulation, the ventilation rate was calculated by determining the mass flow rate at the exhaust shaft. The boundary conditions are labelled in Fig. 2, and the numerical setting is summarized in Table 1.

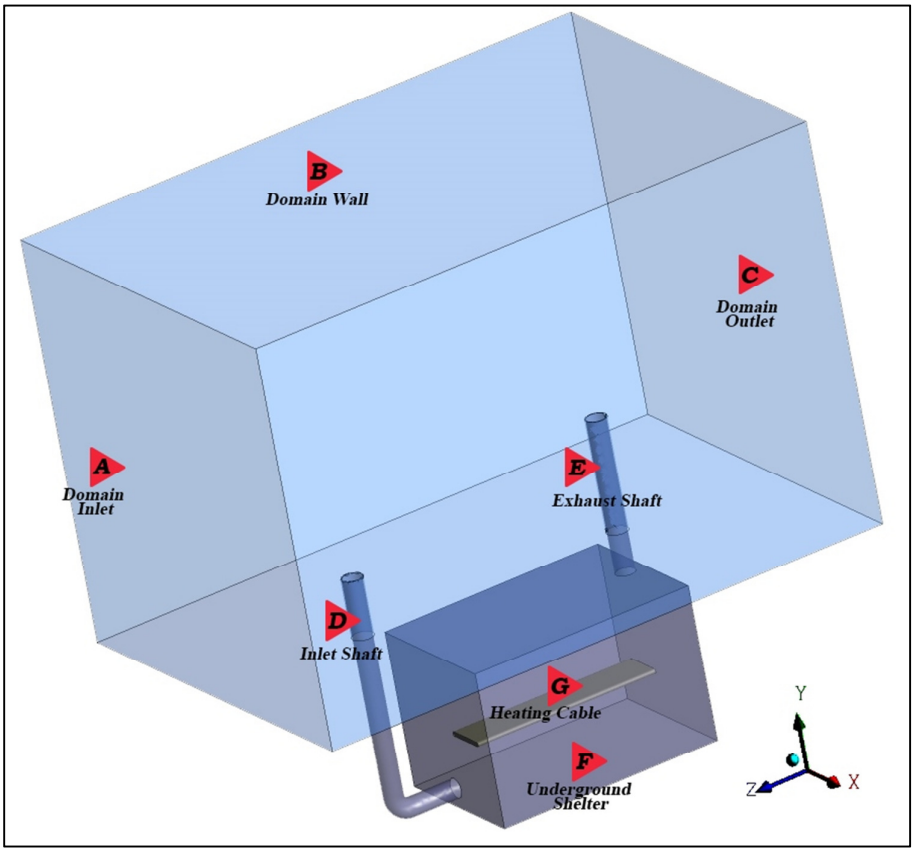

Fig. 2. Boundary Conditions

Table 1
Boundary conditions for the simulation

Domain Inlet	constant velocity, 2.68 m/s at a constant temperature, 23^0C
Domain Outlet	zero pressure
Domain Wall	free slip wall at a constant temperature, 23^0C
Supply Duct	adiabatic, no-slip walls ($u_i = 0$)
Exhaust Duct	adiabatic, no-slip walls ($u_i = 0$)
Heating Cable	heat flux,70 W/m^2
Underground Shelter	adiabatic, no-slip walls ($u_i = 0$)
Domain Outlet	zero pressure

The governing equations of mass (1), momentum (2) and energy (3) conservations are presented below.

$$\frac{\partial \rho}{\partial t} + \nabla . \rho \vec{v} = 0 \tag{1}$$

$$\frac{\partial}{\partial t}(\rho \vec{v}) + \nabla . (\rho \vec{v} \vec{v}) = -\nabla p + \nabla \cdot \bar{\bar{\tau}} + \rho \beta \vec{g} (T - T_o) \tag{2}$$

$$\frac{\partial}{\partial t}(\rho E) + \nabla \cdot \left(\vec{v} (\rho E + p)\right) = -\nabla \cdot (k \nabla T) + \Phi + S_h \tag{3}$$

Here, ρ is density, t is time, $\vec{v}$ is velocity vector, p is pressure, $\bar{\bar{\tau}}$ is the viscous stress tensor, $\vec{g}$ is the gravitational acceleration, E is the total energy, k is the fluid thermal conductivity, T is the absolute temperature, S_h is a source term and Φ is the dissipation function representing the work done by the viscous forces. The terms $\rho \vec{g}$ at the right hand side (RHS) of Equation (2) represents the buoyancy force.

2.2 Goal Driven Optimization

The optimization process was performed by using the Design of Experiment (DOE) and the Response Surface Method (RSM). RSM has been considered due to the well-established surrogate model and easy to operate compare to other surrogate models. Meanwhile, DOE is a systematic way of changing process factors and analysing the response to quantify a cause-effect relationship as well as the random variability of the process by using a minimum number of design points. In this study, the DOE was executed by utilizing the Box-Behnken Design (BBD) method with two-level factorial (see Table 2). BBD is applied in the current study as it can accurately predict the response behaviour and reduce the number of design points which does not contain an embedded factorial design.

As indicated in Fig. 3, three factors were considered for optimization: inlet opening, outlet opening and ratio of elbow shaft (R/H), resulting in 13 design points. A full second-order polynomial of response surface was subsequently used to analyze the aforementioned design points. The second-order polynomial of response surface can be written as [14].

$$\hat{y} = \beta_o + \sum_{i=1}^{k} \beta_i x_i + \sum \sum_{i<j} \beta_{ij} x_i x_j + \sum_{i=1}^{k} \beta_{ii} x_i^2 + \varepsilon \tag{4}$$

Here $\hat{y}$ is the response value, β_o is a constant, β_i and β_j is the coefficient of regression, x is the design variable and, ε is an error term of the estimated model. In the current study, the error term, ε is negligible due to the fact that the model was constructed by using numerical simulation. This equation are estimated via minimizing the sum of squares of the deviation predicted response value $\hat{y}\ (x)$, from the actual response value $y\ (x)$ through the standard least square equation.

$$\beta = [X^T X]^{-1} X^T y \tag{5}$$

where y is the vector of observed response values at all design points and $[X^T X]^{-1}$ exists when X is linearly independent. Thus, the matrix X can be expressed as

$$X_{nxm} = \begin{bmatrix} 1 & x_{11} & \cdots & x_{11}x_{12} & \cdots & x_{1k}^2 \\ \vdots & \vdots & \cdots & \vdots & \ddots & \vdots \\ 1 & x_{n1} & \cdots & x_{n1}x_{n2} & \cdots & x_{nk}^2 \end{bmatrix} \tag{6}$$

Here, $m = (k+1)(k+2)/2$ is the modeling term in the quadratic polynomial. Thus the predicted values at the original design points may differ from the observed values at the designed points. Shifted-Hammersley Sampling (screening algorithm) [15] on the other hand, was utilized to optimize the defined objective function. In the current study, we are interested to maximize the ventilation rate inside the underground shelter. A total of 1000 distributed sample sets are generated within the optimization domain for the screening algorithm.

Table 2
Quantification of Factor and Response Parameters

Parameters		Name	Upper Bound (m)	Lower Bound (m)	Constraints
Factors	P1	Inlet Opening (D1)	0.1524	0.1016	-
	P2	Ratio of Elbow Shaft (R/H)	2.50	0.75	R/H ≥ 0.75
	P3	Outlet Opening (D2)	0.1524	0.1016	-
Response	P4	Ventilation Rate (m^3/s)			

*R/H = radius/height

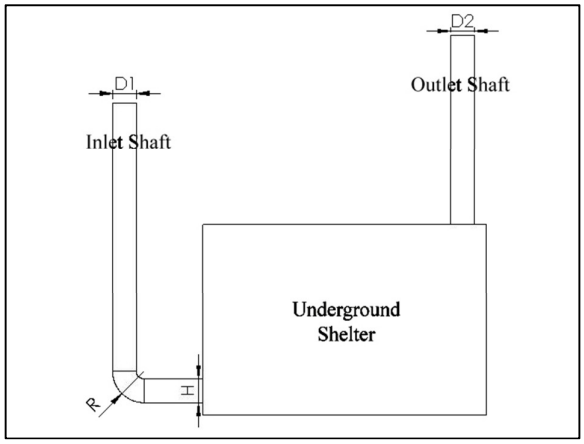

Fig. 3. Optimization parameters

3. Results and Discussion

3.1 Verification and Validation

Before assessing the response surface analysis, the CFD results were compared with the previous experimental result [8]. Grid independence study was firstly performed by utilising six different meshes. Fig. 4 indicates the radial velocities (at the exhaust shaft) obtained by using the two larger mesh sizes namely 1.63 and 2.39 million cells, are comparable. Therefore, the mesh size of case employing 1.63 million cells will be used for subsequent analysis. The model of Grid E was then selected for subsequent flow analysis. Next, a systematic validation of the CFD model was performed. The simulated ventilation rate was 0.0460 m^3/s which is quite close to the measured ventilation rate reported by King [8] (i.e. 0.0477 m^3/s). The percentage difference between these two values is merely 4.4% indicating that the current CFD model is reliable.

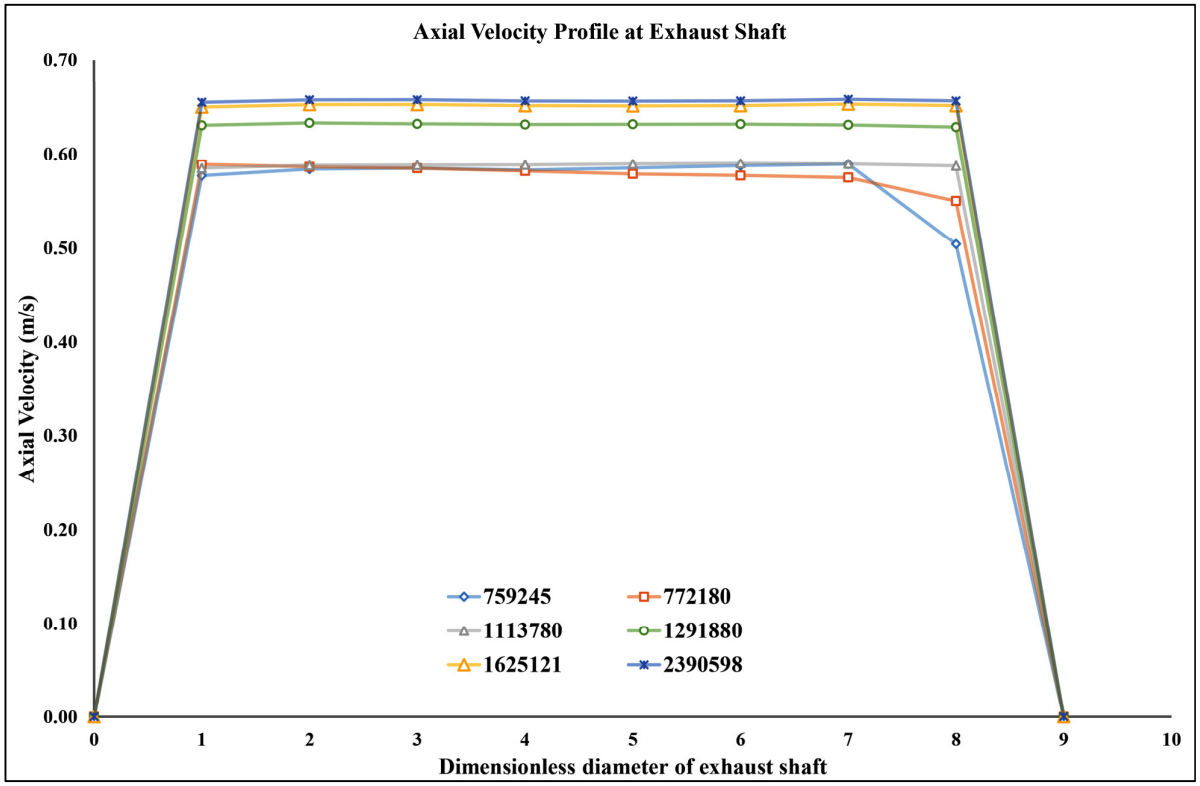

Fig. 4. Grid Independence Test

Besides, Fig. 5 shows the streamline of the airflow from the inlet towards the outlet shaft which exhibits the natural ventilation for the CFD model is working well. Detailed validation studies on the current CFD model can be found as reported by Mukhtar *et al.,* [16].

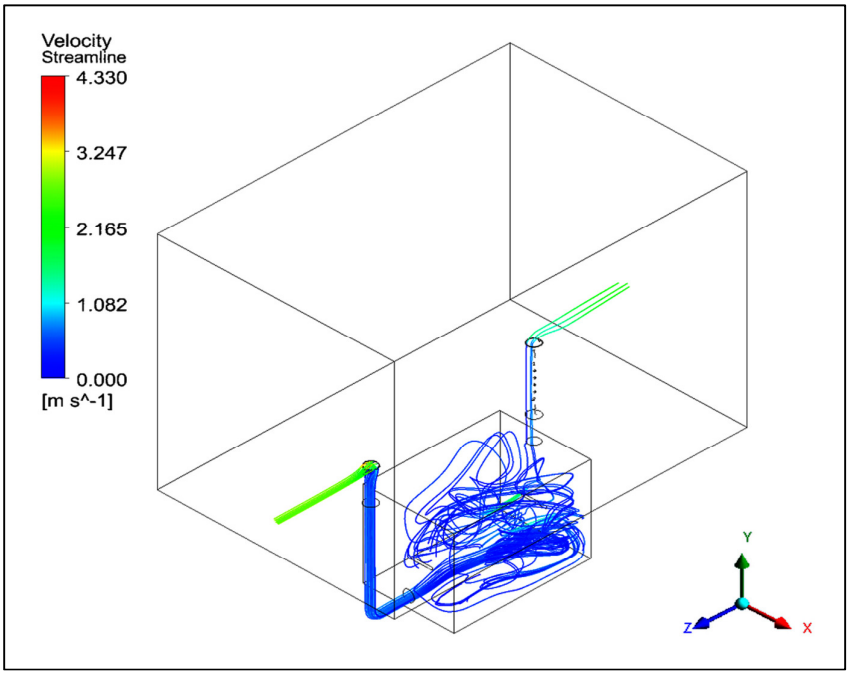

Fig. 5. Indoor Airflow Streamline

3.2 Parameter Correlation

A correlation matrix was constructed to determine the level of correlation between factors and the response. It was obtained by using the Pearson's rank correlation whereby 100 samples with 5% of the relevant threshold are required for filtering the correlation value. As observed from Fig. 6, the ventilation rate is dependent heavily on the outlet opening with 74.09% correlation, followed by an inlet opening with 28.64% and the ratio of elbow shaft with only 0.12%.

1) Linear trend line

$$y = 85.106x + 2.4884 \quad (7)$$

2) Quadratic trend line

$$y = -3933.2x^2 + 321.32x - 0.93207 \quad (8)$$

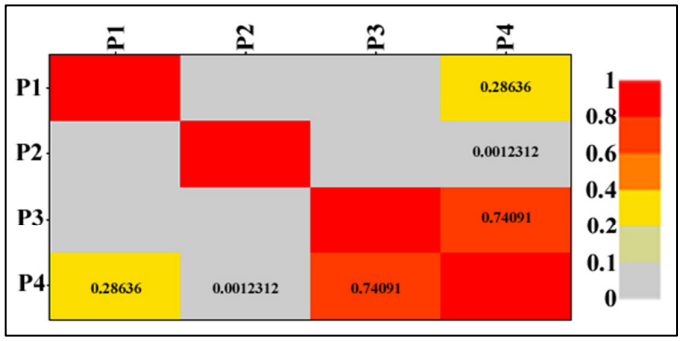

Fig. 6. Correlation matrix

Therefore, inlet and outlet opening are treated as major input parameters (strong correlation) while the ratio of elbow shaft is treated as minor input parameter (weak correlation) which contributes to 96% of the full model of R^2 (see Fig. 7). Besides that, the scatter plot in Fig. 8 was produced to generate the linear and quadratic trend lines. The mathematical model for these trend lines are expressed as follows.

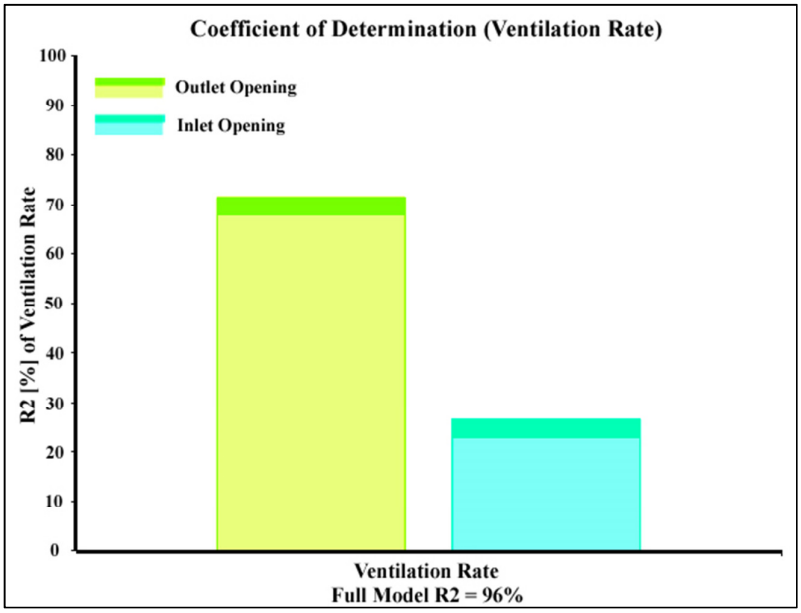

Fig. 7. Coefficient of determination

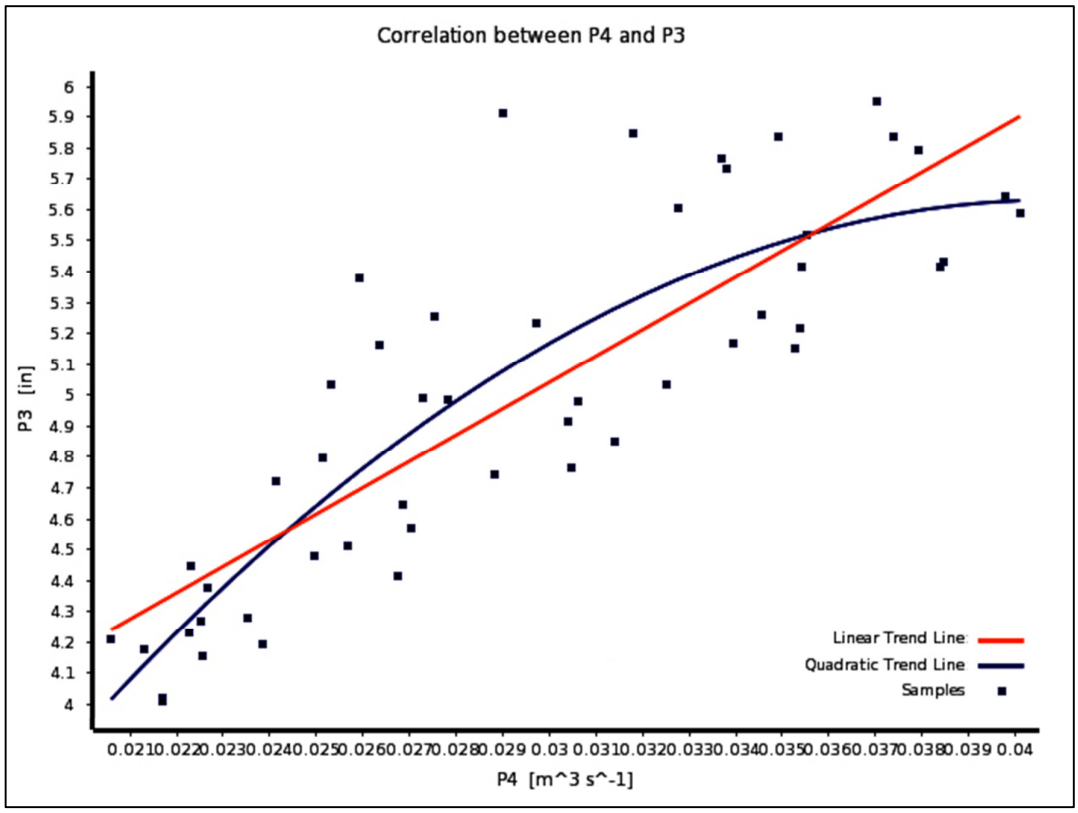

Fig. 8. Scatter plot

3.3 Response Surface Analysis

After simulating the 15 design points via Ansys Design Explorer, the simulation ventilation rate was used to find the quadratic regression model. It is interesting to note that predicted value obtained by quadratic regression model agreed well with the CFD values (see Fig. 9). Likewise, in Fig. 10, the coefficient of determination (R^2) of 99.38% is in reasonable agreement with the adjusted coefficient of determination (R^2) of 99.22%, thus indicating a well-represented response surface. The mathematical model for predicting the Ventilation Rate (VR) can be expressed as follows.

$$VR = -0.038 - 0.00046A - 0.000036B + 0.00161C - 0.001788A^2 - 0.000028B^2 - 0.001651C^2 + 0.000126AB + 0.004310AC - 0.000065BC \quad (9)$$

where *A* is the inlet opening, *B* is the outlet opening, and *C* is the ratio of elbow shaft. This equation can be used to study the response of *VR* by varying the involved parameters. For example, the positive coefficients associated with the factors *C, AB* and *AC* reveal increased ventilation rate if the factors are increased. Conversely, the negative coefficients associated with factors *A, B,* A^2, B^2, C^2 and *BC* indicate decreased ventilation rate when these factors are increased.

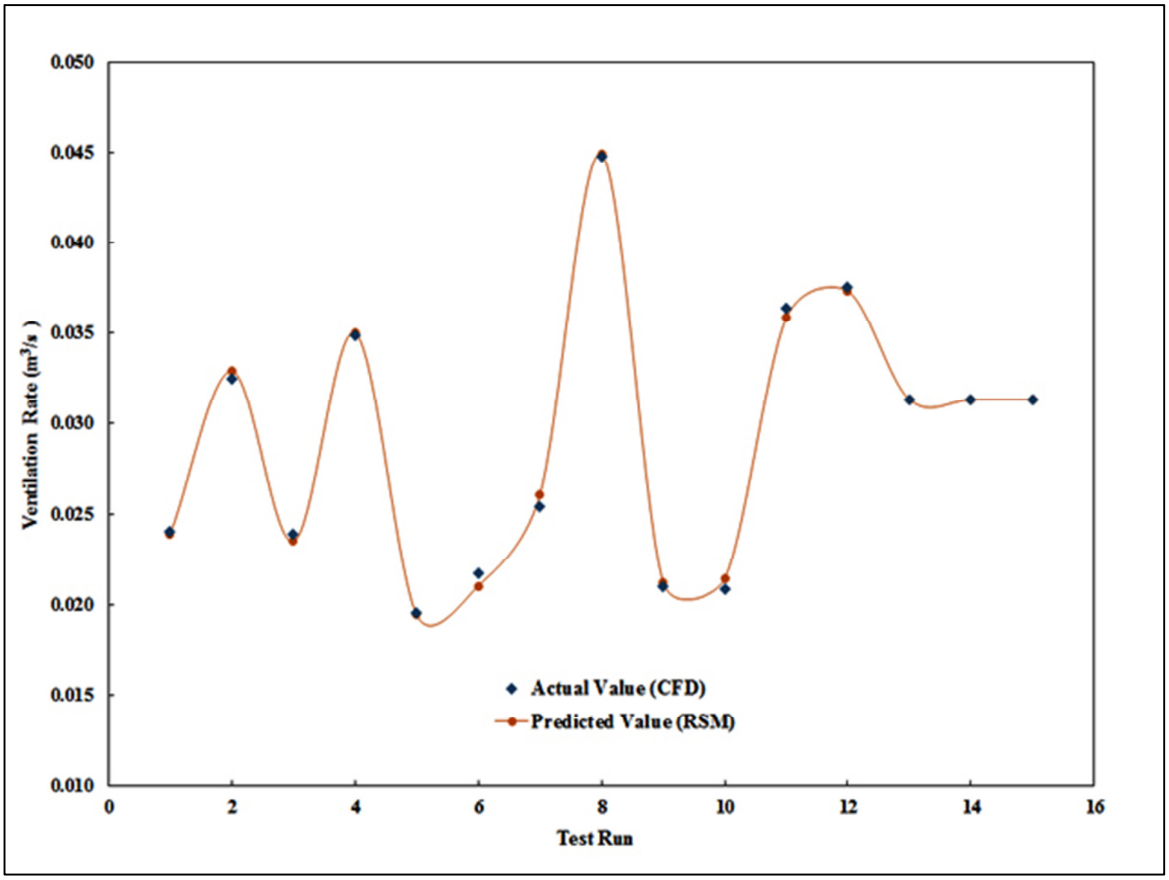

Fig. 9. Comparison between CFD and RSM

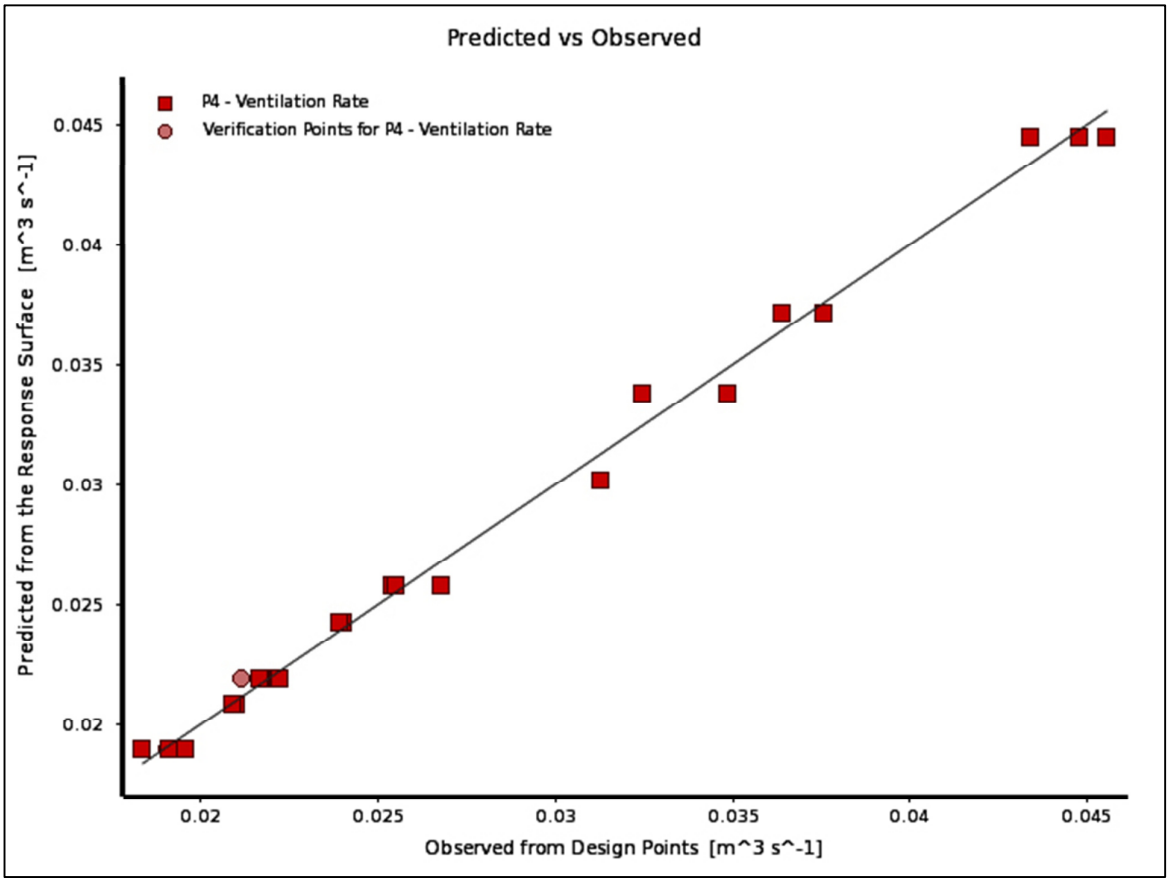

Fig. 10. Quality of fit between predicted and observed point

3.4 Optimization

In order to improve the ventilation rate, the optimization process was undertaken by considering parameters P1, P2 and P3 over the limited ranges based on the previous literature [8]. It was conducted using the Shifted-Hammersley Sampling (screening algorithm) to maximize the ventilation rate (objective function), subject to the constraint of ratio of elbow shaft such as $R/H \geq 0.75$. Fig. 11 indicates that the outlet opening is the most sensitive design parameter, followed by the inlet opening. Fig. 12 shows that the highest ventilation rate can be obtained if the inlet and outlet diameters are high, which can be seen at the top right corner of the contour plot. This optimization also provides three candidate design points that show the best behaviour based on the objective function and constraint (see Table 3). The results indicate that the highest ventilation rate is obtained when the inlet and outlet openings are equal in size. Similar finding has been reported by Edward and Randall [17].

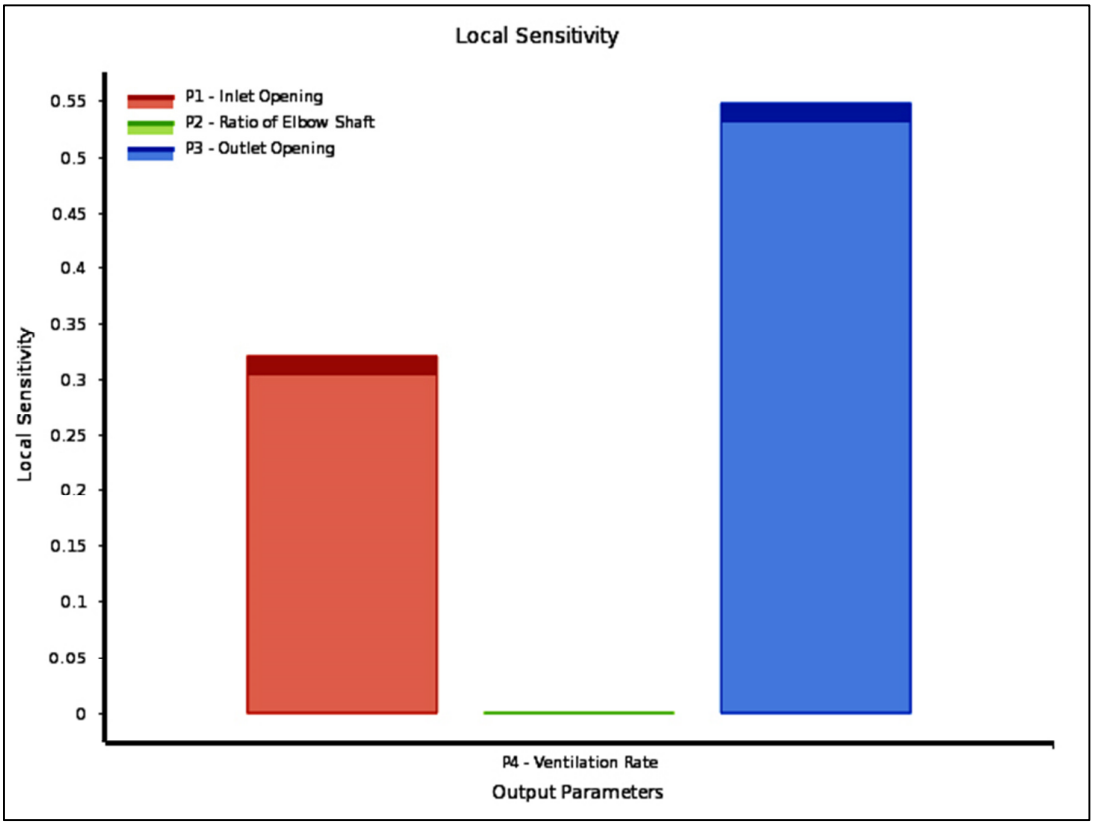

Fig. 11. Sensitivities of the three parameters

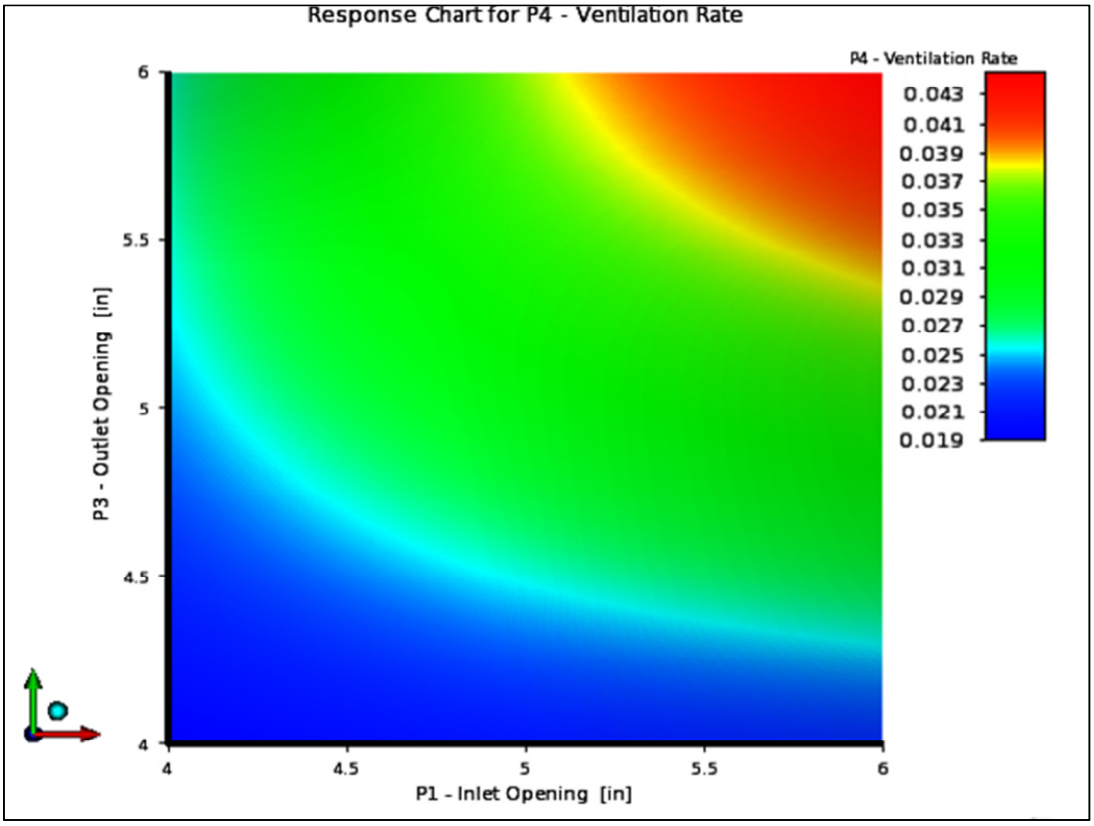

Fig. 12. Response of two major inputs on ventilation rate

Table 3
Candidate points generated from the screening algorithm

Candidate Point	Inlet Opening (m)	Outlet Opening (m)	Ratio of Elbow Shaft (R/H)	Ventilation Rate ($m^3 s^{-1}$)	Variation from references (% differences)
CP 1	0.1524	0.1524	0.833	0.04453	2.24%
CP 2	0.1509	0.1522	1.538	0.04413	3.11%
CP 3	0.1522	0.1506	1.172	0.04394	3.53%

4. Conclusions

A CFD model of underground shelter has been verified and validated with the results obtained from the previous literature. A goal-driven optimization has been conducted as well for increasing the ventilation rate, which it was obtained by using the combination: 0.1524m opening for inlet and outlet and 0.833 for the ratio of elbow shaft (R/H) characteristics (best-optimized conditions). It is interesting to note that the optimization objective of increasing the ventilation rate is achievable. It has been found that the ventilation rate is very sensitive to the diameter of opening outlet. ANSYS Workbench (CFD), integrated with ANSYS Design Exploration (GDO), has been found to be useful for the current optimization study. Potentially, the roles of inlet and outlet positions in ventilation efficiency can be assessed.

Acknowledgement
This study was supported by a scholarship provided by Yayasan Tenaga Nasional (YTN) to the first author.

References
[1] Daghigh R. "Assessing the thermal comfort and ventilation in Malaysia and the surrounding regions." *Renewable and Sustainable Energy Reviews* 48 (2015): 682–91.
[2] Yu W, Li B, Jia H, Zhang M, Wang D. "Application of multi-objective genetic algorithm to optimize energy efficiency and thermal comfort in building design." *Energy and Buildings* 88 (2015): 135–43.
[3] Li Y, Heiselberg P. "Analysis methods for natural and hybrid ventilation – a critical literature review and recent developments." *International Journal of Ventilation* 1 (2003): 3–20.
[4] Mukhtar A, Ng KC, Yusoff MZ. "Passive thermal performance prediction and multi-objective optimization of naturally-ventilated underground shelter in Malaysia." *Renewable Energy* 123 (2018): 342–52.
[5] Goel RK, Singh B, Zhao J. "Underground Infrastructures: Planning, Design, and Construction."(2012).
[6] Holthusen TL. "The potential of earth-sheltered and underground space: Today's resource for tomorrow's space and energy viability." (2013).
[7] Barber ME, Kusuda T, Reynolds PJ, Powell FJ. "A study of air distribution in survival shelters using a small-scale modeling technique." (1972).
[8] King JC. "Gravity ventilation of underground shelters." (1965).
[9] Mukhtar A, Ng KC, Yusoff MZ. "Development and validation of the CFD model for natural ventilation of underground shelter". *Science International Journal* 29 (2017): 521–5.
[10] ANSYS Fluent. Release 15.0. Theory Guide (2013): 1–514.
[11] Etheridge D. "Natural Ventilation of Buildings: Theory, Measurement and Design." *John Wiley & Sons Ltd*. (2012).
[12] Hajdukiewicz M, Geron M, Keane MM. "Calibrated CFD simulation to evaluate thermal comfort in a highly-glazed naturally ventilated room." *Building and Environment* 70 (2013): 73–89.
[13] Liu KS, Sheu TWH, Hwang YH, Ng KC. "High-order particle method for solving incompressible Navier–Stokes equations within a mixed Lagrangian–Eulerian framework." *Computer Methods in Applied Mechanics and Engineering* 325 (2017): 77–101.
[14] Myers RH, Montgomery DC, Anderson-cook CM. "Response Surface Methodology: Process and product optimization using designed experiments." *John Wiley & Sons Ltd.* (2009).
[15] Diwekar UM, Kalagnanam JR. "Efficient Sampling Technique for Optimization under Uncertainty." *AIChE Journal* 43 (1997): 440–7.

[16] Mukhtar A, Ng KC, Yusoff MZ. "Design optimization for ventilation shafts of naturally-ventilated underground shelters for improvement of ventilation rate and thermal comfort." *Renewable Energy* 115 (2018): 183–98.
[17] Edward EJ, Randall WC. "The Neutral Zone in Ventilation." *Transactions of the American Society of Heating and Ventilating Engineers* 32 (1926): 59–74.